analytical chemistry

pubs.acs.org/ac Article

Click Chemistry-Mediated Particle Counting Sensing via Cu(II)-Polyglutamic Acid Coordination Chemistry and Enzymatic Reaction

Zhilong Wang, Luyu Wei, Lingwen Zeng, Niu Feng, Jianjun Chen, and Yiping Chen*

Cite This: *Anal. Chem.* 2022, 94, 5293−5300 Read Online

ACCESS | Metrics & More | Article Recommendations | Supporting Information

ABSTRACT: An electrical resistance-based particle counter (ERPC) with simple operation and high resolution has proved to be a promising biosensing toolkit, whereas amplification-free ERPC biosensors are incapable of analyzing trace small molecules due to their relatively low sensitivity. In this work, click chemistry-mediated particle counting sensing of small-molecule hazards in food samples with high sensitivity was developed. In this strategy, unbound alkyne-functionalized polystyrene microspheres were collected by magnetic separation from the copper-ion-mediated click reaction between alkyne-functionalized polystyrene microspheres and azido-functionalized magnetic beads, which could be used as signal probes for the readout. This click chemistry-mediated ERPC biosensor converts the detection of targets to the quantification of copper ions or ascorbic acid by performing competitive immunoassay-based coordination chemistry and enzymatic reaction, respectively. The sensitivity of the ERPC biosensor has been improved by an order of magnitude due to the signal amplification effects of click chemistry, coordination adsorption, and enzyme catalysis. Furthermore, because of the efficient separation and enrichment of immunomagnetic beads and the robustness of click chemistry, the interference from food matrixes and immunoassay is effectively reduced, and thus, our strategy is exceedingly suitable for detecting trace targets in complex samples.

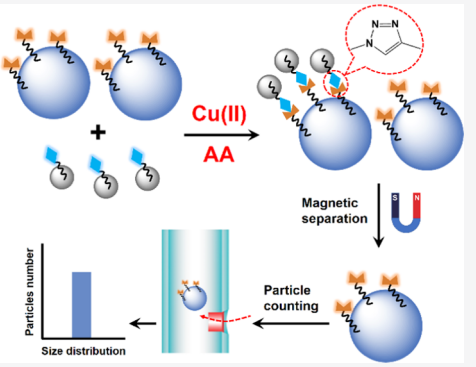

1. INTRODUCTION

Food contamination occurs often and may involve relatively small batches of food or very large ones, where millions of tons of food must be discarded.[1,2] During food production, preservation, distribution, and consumption, it is possible to introduce hazardous substances, leading to great public health risks.[3] For example, the use of pesticides during the cultivation of fruits and vegetables may result in excessive pesticide residues and increase the risk of cancer for consumers.[4,5] Therefore, the availability of safe and pollution-free food is an ongoing and long-term requirement. To meet increasingly rigorous food safety standards, it is crucial and indispensable to explore highly sensitive, easy-to-use, rapid, and inexpensive detection techniques for monitoring food quality and ensuring food security. In addition, the accurate and timely assessment of food quality is of great significance to prevent needless food wastage and enormous economic losses.

Current commercial detection platforms used in the field of food safety mainly include enzyme-linked immunosorbent assay (ELISA) and lateral flow immunoassay (LFIA).[6−8] The bottleneck for LFIA is low sensitivity and poor matrix tolerance, which limits its application. Compared with LFIA, ELISA employs enzymes to amplify detection signals, but its sensitivity is still incapable of detection of hazardous factors at trace levels. In our previous work, an electronic particle counter-implemented versatile biosensing toolkit was developed for detecting a range of targets including protein biomarkers, small molecules, pathogenic bacteria, and even cells.[9] In this sensing strategy, magnetic beads (MBs) coupled with antibodies or molecular probes were employed to capture the target of interest, and polystyrene (PS) microspheres coupled with recognition elements were used as signal probes to detect the target. After the occurrence of molecular events, the unbound signal probes can be rapidly separated and accurately counted by an electrical resistance-based particle counter (ERPC), which can be used to quantify the amount of target. Based on this principle, the highly sensitive detection of biomarkers and foodborne pathogens was achieved using antigen−antibody interaction and DNA hybridization, but the sensitivity was limited to the detection of small molecules because there is only one existing binding site between the antigen and antibody of small molecules.[10] To address this issue, 10 μm PS microspheres were applied to increase the sensitivity due to its greater resistance that can be measured by ERPC. However, the suspension stability of 10 μm PS microspheres is inferior to that of 3 μm PS microspheres,

Received: November 26, 2021
Accepted: March 15, 2022
Published: March 23, 2022

https://doi.org/10.1021/acs.analchem.1c05127
Anal. Chem. 2022, 94, 5293−5300

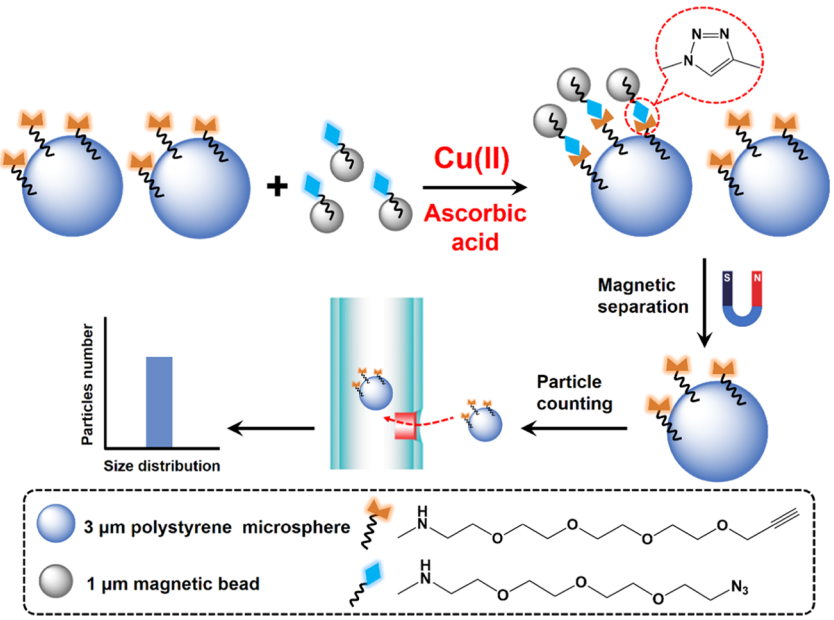

Figure 1. Schematic illustration of the Cu(I)-catalyzed azide/alkyne cycloaddition (CuAAC)-mediated electrical resistance-based particle counter (ERPC) sensing strategy. In this strategy, Cu(II) and ascorbic acid can be used as variables to establish quantitative relationships with other targets using competitive immunoassay-based coordination chemistry and enzymatic reaction.

which increases the difficulty of the operation and decreases the accuracy of the analysis. Therefore, it is necessary to develop an efficient signal amplification strategy to increase the sensitivity of the ERPC biosensor and meet the requirements for trace food hazards analysis.

In this study, a click chemistry-mediated ERPC biosensor was explored for highly sensitive detection of multiple targets such as pesticide residues and mycotoxins. The alkyne-functionalized PS microspheres and azido-functionalized MBs were first prepared using EDC/NHS chemistry. Next, Cu(II) and ascorbic acid (AA) were introduced to trigger Cu(I)-catalyzed azide/alkyne cycloaddition (CuAAC), which integrates the modified PS microspheres and MBs. After magnetic separation, the unbound PS microspheres were subjected to micropore, and the number of particles was counted by the ERPC (Figure 1). In this sensing strategy, the number of microspheres can reflect the amount of Cu(II) or AA in samples, which is the basis of quantitative analysis of this sensing strategy. In addition, the number of unbound microspheres can be regulated by changing the amount of Cu(II) or AA using coordination chemistry and immunoassay, and thus, the detection of targets of interest can be logically transformed into the quantification of Cu(II) or AA.[11−13] For instance, alkaline phosphatase, a labeling enzyme in immunoassays, can catalyze ascorbic acid phosphate to generate AA *via* dephosphorylation.[14] This process can be used to develop the sensing analysis of aflatoxin B_1 by competitive immunoassay. Compared with our previous work, the sensitivity of this sensing strategy is expected to be high due to the signal amplification of click chemistry, coordination adsorption, and enzyme catalysis. Because this sensing strategy can also effectively eliminate the interference of nonspecific absorption by magnetic separation and click reaction, it is highly feasible for usage in real-world settings. Overall, a convenient, robust, highly sensitive, and multifunctional click chemistry-mediated ERPC sensing platform is proposed, which endows it with the ability to detect any small molecule in a complex sample at ultralow concentrations.

2. EXPERIMENTAL SECTION

2.1. Experimental Procedure for Assaying Cu(II). Alkyne-PS microspheres (40 μg mL^{-1}, 100 μL) were mixed with azido-MBs (0.4 mg mL^{-1}, 100 μL); 100 μL of Cu(II) solutions with specific concentration was added into the above mixture; and 100 μL of ascorbic acid (AA) was added to a final concentration of 1.0 mM. After gently shaking the mixture for 10 min, the unbound alkyne-PS microspheres were collected via magnetic separation for signal readout. The measurement procedure was carried out according to our previous work as follows: the signal value of normal saline was measured as background, 100 μL of the collected solution was added to measure the particle number. Particles with a size distribution of 2.6−3.7 μm are counted as 3 μm microspheres, whose average size is 3 μm.[9] LOD was calculated based on the calibration curve with $3S/M$, where S is the value of the standard deviation of blank samples and M is the slope of the standard curve at a low-concentration range.

2.2. Detection of Chlorpyrifos. To evaluate the performance of this biosensing platform for detecting chlorpyrifos, methanol was used to dissolve chlorpyrifos to prepare a stock solution, then a series of chlorpyrifos solutions were mixed with MB-Ab (100 μL), respectively. The final concentration of chlorpyrifos ranged from 0 to 1000 ng mL^{-1}. The mixture solution was softly stirred at room temperature for 20 min. After washing the complex three times by washing buffer, the PGA-PS-Ag was added to incubate with the unused MB-Ab for 30 min to enable the production of immune complex. Then, the immune complex (MB-Ab-chlorpyrifos and PGA-PS-Ag-MB-Ab) was obtained by magnetic separation and resuspended by Cu^{2+} solution (1 mM, 500 μL) to react at room temperature for 20 min. After the interaction between PGA-PS-Ag-MB-Ab and Cu(II) and washing, the excess AA (1 mM) was added to ensure the reduction of remaining Cu(II) to

https://doi.org/10.1021/acs.analchem.1c05127
Anal. Chem. 2022, 94, 5293−5300

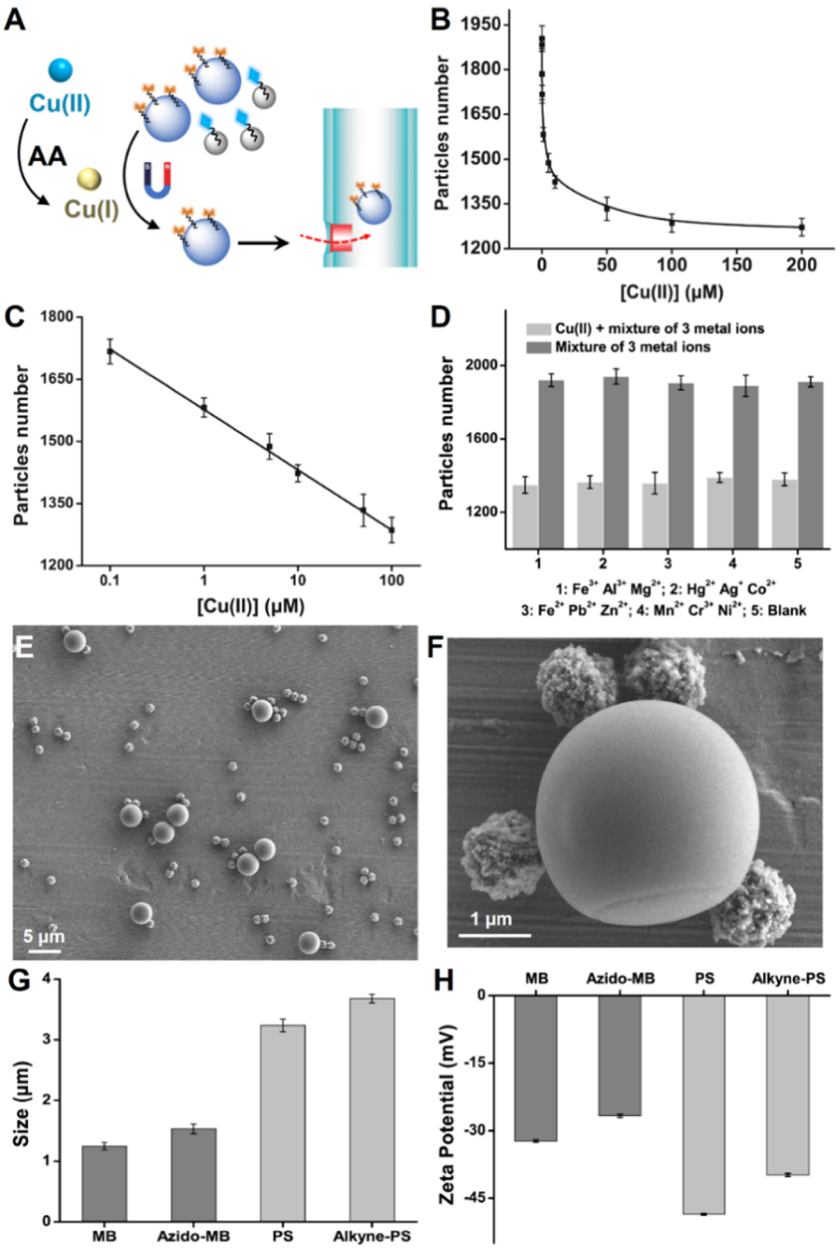

Figure 2. Click chemistry-mediated ERPC assay for sensing of Cu(II). (A) Scheme of click chemistry-mediated ERPC assay for sensing of Cu(II). (B) Standard curve and (C) linear range for detection of Cu(II). (D) Evaluation of anti-interference ability for sensing of Cu(II). The final concentration is 20 μM for Cu(II) and 200 μM for the others. Detailed ions are listed at the bottom. (E, F) Scanning electron microscopy (SEM) images of the conjugate of alkyne-PS microspheres and azido- MBs after the CuAAC reaction. (G) Hydrodynamic size change and (H) ζ potential of MBs, azido-MBs conjugate, PS microspheres, and alkyne-PS microspheres conjugate. Error bars represent the standard deviation of three measurements (n = 3).

Cu(I). Cu(I) then can catalyze the CuAAC between alkyne-PS microsphere and azido-MB, and after magnetic separation, the unbound alkyne-PS microsphere was collected for signal readout. The measurement procedure was the same as above. The concentration of chlorpyrifos in real samples was obtained using the linear equation of the relationship between [chlorpyrifos] and particles number.

2.3. Sensing of AA. Various concentrations of AA were mixed with Cu(II), alkyne-PS microspheres, and azido-MBs to incubate at room temperature for 10 min, and the particle number of separated solutions was measured by ERPC.

2.4. Sensing of ALP. ALP was mixed with 2-phospho-L-ascorbic acid trisodium salt (AAP) (20 mM, 20 μL) and Tris-HCl buffer (0.05 M, 60 μL, pH 7.4), and the final concentrations of ALP ranged from 0.05 to 500 U L^{-1}. The mixture solution was incubated for 1 h at 37 °C. After that, the mixture solution was instantly added to the centrifuge tube that included Cu(II) (1 mM, 100 μL), alkyne-PS microsphere (40 μg mL^{-1}, 100 μL), and azido-MB (0.4 mg mL^{-1}, 100 μL) for the CuAAC reaction. After magnetic separation, the unbound alkyne-PS microspheres were collected for signal readout. The measurement procedure was the same as above.

2.5. Detection of AFB_1. First, various concentrations of AFB_1 antigen were incubated with antibodies of AFB_1 at 37 °C for 20 min, respectively. Next, 50 μL of MBs-bovine serum albumin (BSA)-AFB_1 conjugate was added to the above

https://doi.org/10.1021/acs.analchem.1c05127
Anal. Chem. 2022, 94, 5293−5300

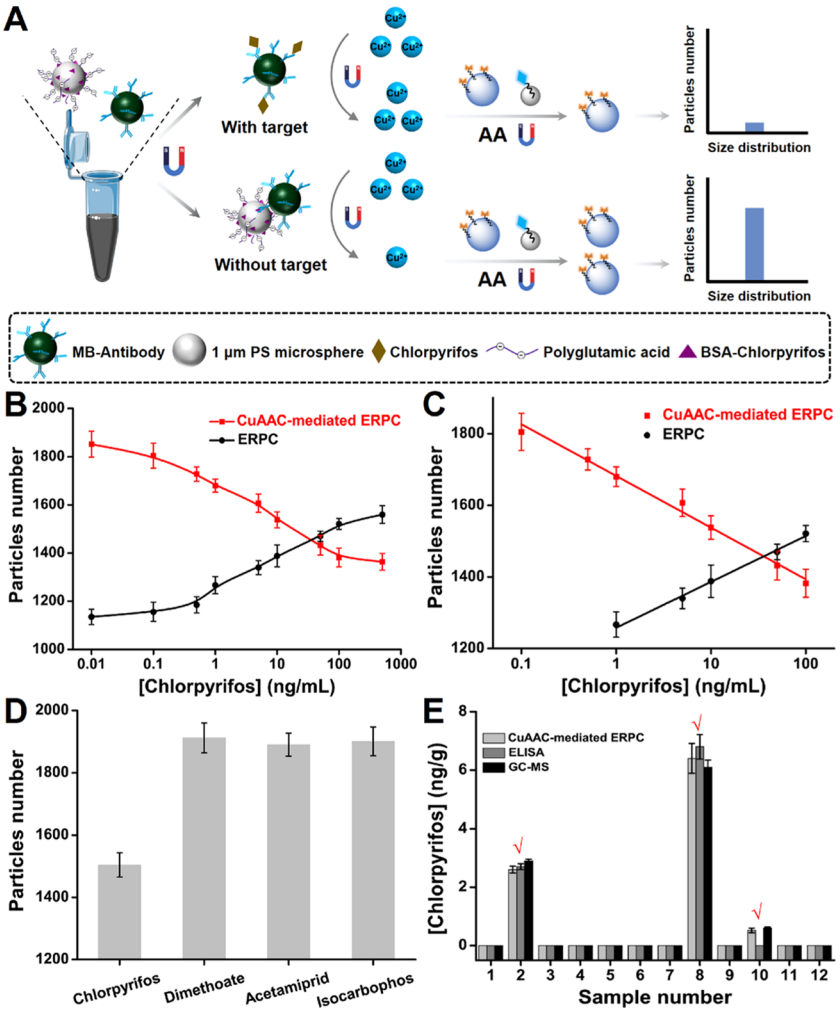

Figure 3. Detection of chlorpyrifos by CuAAC-mediated ERPC biosensor via Cu(II)-polyglutamic acid (PGA) coordination chemistry. (A) Scheme of Cu(II)-PGA coordination chemistry-based CuAAC-mediated ERPC immunoassay for detection of chlorpyrifos. (B) Standard curve, (C) linear range, and (D) specificity for detection of chlorpyrifos. The concentrations of all analytes are 10 ng mL^{-1}. (E) Comparison of CuAAC-mediated ERPC biosensor, ELISA, and gas chromatography−mass spectrometry (GC-MS) for the detection of chlorpyrifos in apple samples. "√" represents positive samples. Error bars represent the standard deviation of three measurements (n = 3).

mixture solution. Each mixture was gently shaken for 45 min at 37 °C. All of the tubes were then put on a magnetic separation rack for 30 s and washed by PBST (PBS buffer containing 0.5% Tween-20, pH 7.4) three times. ALP-labeled goat anti-mouse IgG conjugate solution (100 μL) was added into the above mixture and shaken at 37 °C for 30 min. After the washing step, AAP (20 mM, 100 μL) was added to the above immune complex for incubating 45 min, and subsequently, the supernatant of each sample was added into the mixture solution of Cu(II) (1 mM, 100 μL), alkyne-PS microsphere (40 μg mL^{-1}, 100 μL), and azido-MB (0.4 mg mL^{-1}, 100 μL) for 10 min. After magnetic separation, the unbound alkyne-PS microspheres were collected for signal readout. The measurement procedure was the same as above.

3. RESULTS AND DISCUSSION

3.1. Sensing of Cu(II) by Click Chemistry-Mediated ERPC Assay. As a proof of concept, this click chemistry-mediated ERPC sensing strategy was initially employed to detect Cu(II), which is generally used as a substrate in CuAAC.[15,16] Given that AA has the reducing ability to convert Cu(II) to Cu(I), this sensing strategy was applied to measure the concentration of Cu(II) in phosphate-buffered saline (PBS) solution by a one-step operation (Figure 2A). To obtain highly sensitive detection of Cu(II), the coupling amount of alkyne ligand molecules, the mass ratio of azido-MBs to alkyne-PS microspheres, the concentration of AA, and the response time of the click reaction were optimized (Figure S1). Under optimized conditions, the number of particles decreased when the concentration of Cu(II) increased from 0 to 200 μM (Figure 2B). Moreover, this sensing strategy exhibited a broad linear range from 0.1 to 100 μM with the linear equation $Y = -145.5\ X + 1576.9$ {X = log [Cu(II) (μM)], R^2 = 0.996}, and the limit of detection (LOD) for Cu(II) by particle number change is as low as 54 nM (S = 47.1, M = 2389.8) (Figure 2C). Notably, the proposed strategy exhibited a more optimal performance for Cu(II) detection than other developed methods (Table S1). The high sensitivity of this sensing strategy is attributed to two main factors: (1) CuAAC increases the efficiency of the binding between functionalized MBs and microspheres;[17,18] (2) the high sensitivity of ERPC for 3 μm PS microspheres that as low as 2 microspheres can be measured.[9] These results indicate that this sensing strategy can detect trace amounts of Cu(II) in aqueous solutions. To

https://doi.org/10.1021/acs.analchem.1c05127
Anal. Chem. 2022, 94, 5293−5300

evaluate the anti-interference ability of this strategy for Cu(II) sensing, the experiment was performed in the presence of mixtures containing three random metal ions. The four groups of mixtures with other metal ions are incapable of influencing the particle number change of the detection system (Figure 2D). These results suggest that this sensing strategy is sufficiently effective so that assays in complex samples can successfully be performed.

To confirm the aggregation at the microscale, scanning electron microscopy (SEM) was utilized to image the alkyne-PS microspheres and azido-MBs after the CuAAC reaction. The SEM images display that the CuAAC reaction results in the azido-MBs gathering around the surface of the alkyne-PS microspheres (Figure 2E,F). The coupling of functional molecules to MBs and PS microspheres was assessed by Fourier transform infrared spectroscopy.[19,20] The absorption bands at approximately 2120 and 2200 cm^{-1} mainly derived from the N═N═N band of azido molecules and the C≡C band of alkyne molecules, respectively (Figure S2). Dynamic light scattering was also employed to characterize the MBs, PS microspheres, and their conjugates. According to the hydrodynamic size distribution results, the sizes of MBs, azido-MBs, PS microspheres, and alkyne-PS microspheres were 1.25, 1.53, 3.24, and 3.68 μm, respectively (Figure 2G). In addition, the ζ potentials of MBs, azido-MBs, PS microspheres, and alkyne-PS microspheres were −32.3, −26.7, −48.55, and −39.85 mV, respectively (Figure 2H). The characterization experiments fully demonstrated the successful coupling of functional molecules to MBs and PS microspheres and the occurrence of click reaction between azido-MBs and alkyne-PS microspheres.

3.2. Detection of Chlorpyrifos in Apple Samples by Click Chemistry-Mediated ERPC Biosensor. Chlorpyrifos, a broad-spectrum organophosphorus insecticide, is widely used to increase crop yield and control pests.[21] However, the residues of chlorpyrifos in food and the environment are major concerns for the public because of the accompanying severe health hazards.[22,23] Thus, the development of a sensitive and specific method is required to detect chlorpyrifos. To investigate the practicability of this sensing strategy, a click chemistry-mediated particle counting immunoassay was employed to detect chlorpyrifos in PBS and apple samples *via* the coordination interaction between Cu(II) and polyglutamic acid (PGA) (Figure 3A). The presence of chlorpyrifos will compete with PGA and complete antigen-functionalized PS microspheres for antibody-labeled MBs. After magnetic separation, the immunocomplex was obtained and cannot change the amount of Cu(II) in the solution. When chlorpyrifos is absent, the PGA-PS-Ag-MB-Ab complex was obtained. The obtained complex can then adsorb Cu(II) in the solution via coordination chemistry between PGA and Cu(II), and after the second magnetic separation, the remaining Cu(II) in the solution can be used to trigger CuAAC between azido-MBs and alkyne-PS microspheres by adding AA. Hence, the number of unbound alkyne-PS microspheres with an average size of 3 μm can be employed to signal readout by ERPC.

The ability of the coordination chemistry-based CuAAC-mediated ERPC immunoassay to detect chlorpyrifos was confirmed by measuring the particle number of the samples with different concentrations of chlorpyrifos from 0.01 to 500 ng mL^{-1} (Figure 3B). To obtain the best analysis performance, the concentration of Ab-MB was first optimized, and the optimal concentration was 0.2 mg mL^{-1} (Figure S3). The LOD is 0.078 ng mL^{-1} (S = 35.2, M = 1369.1), and linear range is from 0.1 to 100 ng mL^{-1}, with a linear equation of $Y = -144.3\ X + 1682$ {X = log [chlorpyrifos (ng mL^{-1})], R^2 = 0.99} (Figure 3C). As a comparison, the ERPC biosensor and conventional ELISA were also used to test for chlorpyrifos. For the ERPC biosensor, the LOD is 0.81 ng mL^{-1} (S = 25.8, M = 95.6) and linear range is from 1 to 100 ng mL^{-1}, with a linear equation of $Y = 128.2X + 1257.9$ {X = log [chlorpyrifos (ng mL^{-1})], R^2 = 0.992} (Figure 3B). For the conventional horseradish peroxidase (HRP)-based ELISA, the LOD is 1.1 ng mL^{-1} (S = 0.0216, M = 0.0589) and the linear range is from 5 to 1000 ng mL^{-1} (Figure S4). Based on our previous work,[12,13] PGA and Cu(II) can be well combined through coordination adsorption and form steady chelates. This is a key factor for productive signal conversion and highly sensitive detection of chlorpyrifos. The high sensitivity and broad linear range of this method allow dilution of the sample as much as possible in practical application to reduce substrate interference and nonspecific binding. The specificity of this sensing strategy was also evaluated. The number of particles from chlorpyrifos measurement was much less than those from dimethoate, acetamiprid, and isocarbophos (Figure 3D), indicating that there is satisfactory selectivity for chlorpyrifos detection with this approach due to the high specificity of CuAAC and antigen−antibody interaction.

The accuracy of this method was assessed by detecting chlorpyrifos in spiked apple samples. The recoveries ranged from 84 to 110% with a coefficient of variations (CVs) from 8.1 to 9.09% (Table S2). The satisfactory recovery and CVs imply that this strategy has great potential for the detection of chlorpyrifos in complex samples. To prove the availability of this method, 12 apple samples were analyzed. For comparison, a screening method (ELISA) and a gold standard method (gas chromatography−mass spectrometry (GC−MS)) were used to detect those samples. It was determined that samples 2, 8, and 10 were positive by the GC-MS method and CuAAC-mediated ERPC biosensor (Figure 3E), indicating that the proposed method has satisfactory consistency with the GC-MS method. However, only sample 2 and sample 8 were positive by ELISA, due to its limited sensitivity. These results validate the capability of the proposed method as a promising tool for trace pesticide residue detection in real-world applications.

3.3. Sensing of Ascorbic Acid by Click Chemistry-Mediated ERPC Assay. To further expand its application, this sensing strategy was used to detect ascorbic acid (AA) (Figure S5A), which is an important reducing agent that converts Cu(II) to Cu(I). As shown in Figure S5B, there was a decrease in the particle number with increasing amounts of AA from 0 to 1000 μM. The LOD for AA by this sensing strategy can reach 0.82 μM (S = 15.7, M = 57.5), with a linear range from 1 to 500 μM, with a linear equation of $Y = -154.5X + 1869.4$ {X = log [AA (μM)], R^2 = 0.997} (Figure S5C). The results demonstrated that the change in the AA-induced particle number has a wide linear range and high sensitivity, which could be applied to develop AA-mediated bioassay.

3.4. Sensing of Alkaline Phosphatase by Click Chemistry-Mediated ERPC Assay. Alkaline phosphatase (ALP) is a hydrolytic enzyme that plays a vital role in many fields, such as immunoassay and disease surveillance.[24,25] Given that 2-phospho-L-ascorbic acid (AAP) can be transformed into AA by ALP-catalyzed dephosphorylation, this principle can be applied to measure the concentration of ALP

https://doi.org/10.1021/acs.analchem.1c05127
Anal. Chem. 2022, 94, 5293−5300

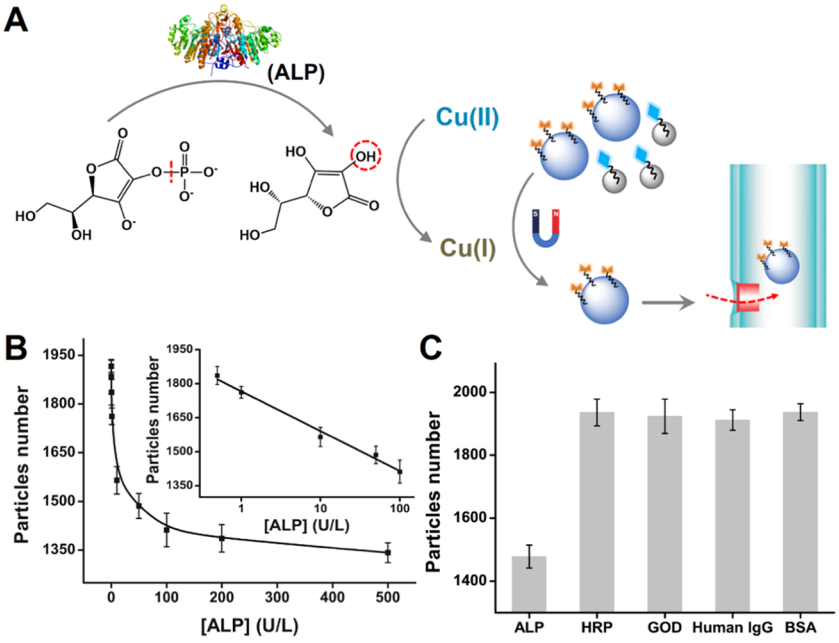

Figure 4. Sensing of ALP by the click chemistry-mediated ERPC assay. (A) Scheme of the click chemistry-mediated ERPC assay for sensing of ALP. (B) Standard curve and linear range and (C) specificity for sensing of ALP. The concentrations of other enzymes and proteins are 100 U L^{-1} and 10 μg mL^{-1}, respectively. Error bars represent the standard deviation of three measurements (n = 3).

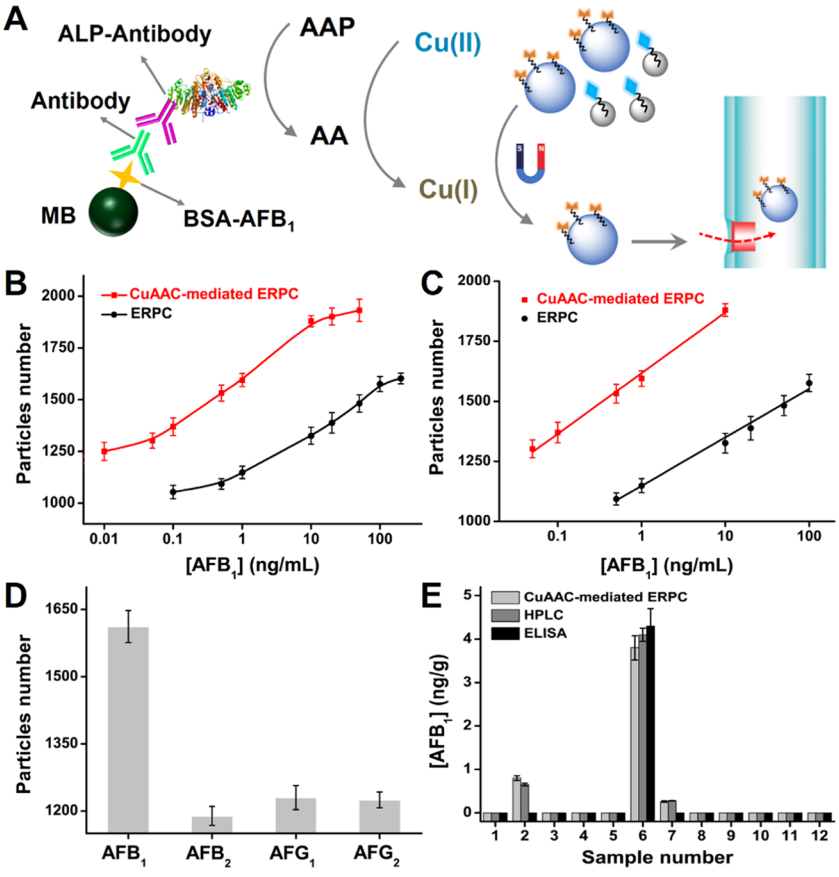

Figure 5. Detection of AFB_1 by CuAAC-mediated ERPC biosensor. (A) Scheme of the CuAAC-mediated ERPC biosensor for detecting AFB_1. (B) Standard curve, (C) linear range, and (D) specificity for detecting AFB_1. The concentration of AFB_1 analogues is 5 ng mL^{-1}. (E) Comparison of the CuAAC-mediated ERPC biosensor, high-performance liquid chromatography (HPLC), and ELISA for detecting AFB_1 in maize samples. Error bars represent the standard deviation of three measurements (n = 3).

through a change in the number of CuAAC-mediated particles (Figure 4A). In this sensing strategy, the change in the particle number value reflects the amount of ALP that could be used for quantitative detection of ALP. The concentration of alkyne-

https://doi.org/10.1021/acs.analchem.1c05127
Anal. Chem. 2022, 94, 5293−5300

PS microspheres was first optimized, and its optimal concentration for signal readout was 40 μg mL^{-1} (Figure S6). As shown in Figure 4B, the particle number gradually decreased when the concentration of ALP ranged from 0 to 500 U L^{-1}. The LOD for ALP detection is 0.35 U L^{-1} (S = 18.6, M = 160.4) and the linear range is from 0.5 to 100 U L^{-1} (Figure 4B). The linear equation is $Y = -175.5X + 1766.5$ with R^2 = 0.987 {X = log [ALP (U L^{-1})]}. To evaluate the specificity of this particle count sensing strategy for ALP detection, a group of other enzymes and proteins (horseradish peroxidase, glucose oxidase, human IgG, and bovine serum albumin) were employed as analogues (Figure 4C). It was found that only ALP can trigger the click reaction and cause a significant change in particle number due to the outstanding specificity of an enzyme to its substrate. These results confirmed that the developed method could be used to detect other targets of interest using ALP as an immunolabeling enzyme. For proof of application, ALP in 12 human serum samples was detected by CuAAC-mediated ERPC assay and conventional p-nitrophenyl phosphate (pNPP)-based method. The CuAAC-mediated ERPC assay has a good coincidence with the pNPP-based method (Figure S7), which proves the reliability of this proposed method in a real-world application.

3.5. Detection of Aflatoxin B$_1$ in Maize by Click Chemistry-Mediated ERPC Biosensor. Aflatoxin B$_1$ (AFB$_1$) is the most common and poisonous mycotoxin of natural origin, and it can contaminate almost all crops, including maize and peanuts. Once contaminated food is ingested, AFB$_1$ can be activated by hepatic cytochrome P450 to form AFB$_1$-8,9-exo-epoxide, which can cause DNA damage and induce aflatoxicosis when it combines with proteins or amino acids.[26−28] Considering its high toxicity and harmfulness, it is necessary to establish a rapid, facile, and highly sensitive method for AFB$_1$ detection. Herein, the particle counting-based sensing strategy can detect AFB$_1$ using ALP-mediated click chemistry (Figure 5A). In the presence of AFB$_1$, it will compete with the bovine serum albumin (BSA)−antigen conjugate coupled on the surface of the MBs for the antibody of AFB$_1$. After magnetic separation and washing steps, the ALP-labeled antibody will be captured by the BSA−antigen−antibody complex on the surface of the MBs, and then, the ALP-triggered click reaction integrated with magnetic separation will change the number of alkyne-PS microspheres in solution. In the absence of AFB$_1$, more antibodies will be bound by the BSA−antigen conjugate followed by additional ALP-labeled antibodies, resulting in fewer alkyne-PS microspheres in solution. Therefore, the number of microspheres in solution is positively correlated with the amount of AFB$_1$.

Based on the described principle, the quantitative detection of AFB$_1$ was performed. In this assay, the optimized concentration of alkyne-PS microspheres for readout was 40 μg mL^{-1} (Figure S8). Under optimal conditions, a concentration-dependent response was obtained, with the concentration of AFB$_1$ from 0.01 to 50 ng mL^{-1} (Figure 5B). The LOD is 34.9 pg mL^{-1} (S = 21.2, M = 1822.6), and the linear range is from 0.05 to 10 ng mL^{-1}, with a linear equation of $Y = 252.8X + 1617.2$ {X = log [AFB$_1$ (ng mL^{-1})], R^2 = 0.995} (Figure 5C). For comparison, the sensitivity and linear range of the ERPC biosensor for sensing AFB$_1$ were studied. The particle number value gradually increased with the concentration of AFB$_1$ from 0.1 to 200 ng mL^{-1} (Figure 5B). The LOD is 0.31 ng mL^{-1} (S = 23.6, M = 227.6), and the linear range is from 0.5 to 100 ng mL^{-1}, with a linear equation of $Y = 201.6X + 1148.1$ {X = log [AFB$_1$ (ng mL^{-1})], R^2 = 0.992} (Figure 5C). Its analysis capability was also compared with conventional ALP-based ELISA using pNPP as the substrate. The LOD of pNPP-based ELISA is 0.17 ng mL^{-1} (S = 0.03, M = 0.533), and the linear range is from 1.0 to 100 ng mL^{-1} (Figure S9). These results show that the proposed strategy outcompetes the ERPC biosensor and ELISA for detecting AFB$_1$. There are greater advantages in using the proposed strategy over the ERPC biosensor and ELISA due to two factors: (1) enzyme amplification effect can produce abundant AA that reduces Cu(II) to Cu(I)[29] and (2) the CuAAC-based bio-orthogonal reaction between alkyne-PS and azide-MB is a highly efficient covalent binding modality, resulting in a significant particle number change and signal amplification.[30,31]

The selectivity of this method was assessed using AFB$_2$, AFG$_1$, and AFG$_2$ as AFB$_1$ analogues to conduct the competitive immunoassay (Figure 5D). The specific interaction between the antibody and AFB$_1$ guarantees a significant change in particle number compared with other analogues, confirming its expected specificity. The accuracy of this strategy was proved by detecting AFB$_1$ in spiked maize. The recoveries ranged from 75.2 to 83.6%, with a CV from 6.8 to 13.9% (Table S3), demonstrating that this strategy has the potential to detect AFB$_1$ in real samples.

To confirm the real-world application of this strategy, a blind test was performed using 12 maize samples. The HPLC method and ELISA were also employed to analyze the same batch of samples. It was determined that samples 2, 6, and 7 were AFB$_1$-positive by the CuAAC-mediated ERPC biosensor and the HPLC method, and the other samples were negative (Figure 5E), indicating that our strategy has the ability equal to that of the HPLC method to detect AFB$_1$ in maize samples. However, only sample 6 tested as AFB$_1$-positive by ALP-based ELISA, suggesting that the accuracy of this strategy for AFB$_1$ detection is greater than that of ELISA due to its higher anti-interference capability. The obvious advantage of our strategy compared with the HPLC method is that it enables accurate and rapid detection of a target at trace level in complicated samples but does not require complex and expensive equipment.

4. CONCLUSIONS

Herein, a click chemistry-mediated ERPC biosensor *via* coordination chemistry and enzymatic reaction is presented, offering a robust and highly sensitive analysis of small-molecule hazards in food samples. This CuAAC-mediated particle count sensing strategy increases the sensitivity of the ERPC biosensor by signal amplification of click chemistry, coordination adsorption, and enzyme catalysis and also widens the application range of the ERPC for testing of food quality. In future work, we will focus on integrating this sensing strategy with microfluidic and microfabrication technology for automation and high-throughput analysis.

■ ASSOCIATED CONTENT

Supporting Information

The Supporting Information is available free of charge at https://pubs.acs.org/doi/10.1021/acs.analchem.1c05127.

Materials and methods; optimization of the coupling amount of alkyne ligand molecules, mass ratio of azido-MBs to alkyne-PS microspheres, concentration of AA,

https://doi.org/10.1021/acs.analchem.1c05127
Anal. Chem. 2022, 94, 5293−5300

and response time of click reaction; Fourier transform infrared spectra of blank MB and azido-MB and blank PS and alkyne-PS; optimization of the concentration of Ab-MB for chlorpyrifos detection; detection of chlorpyrifos by HRP-based ELISA; sensing of AA by click chemistry-mediated particle count assay; optimization of the concentration of alkyne-PS microspheres for ALP detection; comparison of the CuAAC-mediated ERPC assay and conventional pNPP-based method for detecting ALP in human serum samples; optimization of the concentration of alkyne-PS microspheres for AFB_1 detection; detection of AFB_1 by ALP-based ELISA; comparison of the proposed strategy and other developed methods for Cu(II) detection; recoveries of chlorpyrifos from apples at different concentration levels; and recoveries of AFB_1 from maize at different concentration levels (PDF)

AUTHOR INFORMATION

Corresponding Author

Yiping Chen − *Key Laboratory of Environment Correlative Dietology, Huazhong Agricultural University, Ministry of Education, Wuhan 430070, China; Shenzhen Branch, Guangdong Laboratory for Lingnan Modern Agriculture, Genome Analysis Laboratory of the Ministry of Agriculture, Agricultural Genomics Institute at Shenzhen, Chinese Academy of Agricultural Sciences, Shenzhen 518120, China;* orcid.org/0000-0001-9309-2730; Email: chenyiping@mail.hzau.edu.cn

Authors

Zhilong Wang − *Key Laboratory of Environment Correlative Dietology, Huazhong Agricultural University, Ministry of Education, Wuhan 430070, China*

Luyu Wei − *Key Laboratory of Environment Correlative Dietology, Huazhong Agricultural University, Ministry of Education, Wuhan 430070, China*

Lingwen Zeng − *Wuhan Zhongke Zhikang Biological Technology Co., Ltd., Wuhan 430074, China*

Niu Feng − *Key Laboratory of Environment Correlative Dietology, Huazhong Agricultural University, Ministry of Education, Wuhan 430070, China*

Jianjun Chen − *Wuhan Shangcheng Biotechnology Co., Ltd., Wuhan 430063, China*

Complete contact information is available at: https://pubs.acs.org/10.1021/acs.analchem.1c05127

Notes

The authors declare no competing financial interest.

ACKNOWLEDGMENTS

The authors thank the Laboratory of Lingnan Modern Agriculture Project (NZ2021036), the Fundamental Research Funds for the Central Universities (2662020SPPY014), the HZAU-AGIS Cooperation Fund (SZYJY2021002), and Hubei Hongshan Laboratory for financial support.

REFERENCES

(1) da Luz, S. R.; Villanova, F. A.; Rockembach, C. T.; Ferreira, C. D.; Dallagnol, L. J.; Fernandes Monks, J. L.; de Oliveira, M. *Food Chem.* **2022**, *372*, No. 131174.

(2) Djekic, I.; et al. *Food Control* **2021**, *122*, No. 107800.

(3) Tralau, T.; Oelgeschlager, M.; Kugler, J.; Bloch, D.; Braeuning, A.; Burgdorf, T.; Marx-Stoelting, P.; Ritz, V.; Schmeisser, S.; Trubiroha, A.; Zellmer, S.; Luch, A.; Schonfelder, G.; Solecki, R.; Hensel, A. *Nat. Food* **2021**, *2*, 463−468.

(4) Tang, F. H. M.; Lenzen, M.; McBratney, A.; Maggi, F. *Nat. Geosci.* **2021**, *14*, 206.

(5) Möhring, N.; Ingold, K.; Kudsk, P.; Martin-Laurent, F.; Niggli, U.; Siegrist, M.; Studer, B.; Walter, A.; Finger, R. *Nat. Food* **2020**, *1*, 535−540.

(6) Rodriguez, R. S.; O'Keefe, T. L.; Froehlich, C.; Lewis, R. E.; Sheldon, T. R.; Haynes, C. L. *Anal. Chem.* **2021**, *93*, 23−40.

(7) Abdolmaleki, K.; Khedri, S.; Alizadeh, L.; Javanmardi, F.; Oliveira, C. A. F.; Khaneghah, A. M. *Trends Food Sci. Technol.* **2021**, *115*, 500−511.

(8) Xiao, X.; Hu, S.; Lai, X.; Peng, J.; Lai, W. *Trends Food Sci. Technol.* **2021**, *111*, 68−88.

(9) Wang, Z.; Liu, J.; Yang, Y.; Li, P.; Li, K.; Xianyu, Y.; Chen, Y.; Li, B. *Anal. Chem.* **2021**, *93*, 6178−6187.

(10) Toh, S. Y.; Citartan, M.; Gopinath, S. C. B.; Tang, T.-H. *Biosens. Bioelectron.* **2015**, *64*, 392−403.

(11) Dong, M.; Zheng, W.; Chen, Y.; Xianyu, Y.; Ran, B.; Qian, Z.; Jiang, X. *Anal. Chem.* **2018**, *90*, 9148−9155.

(12) Wu, J.; Xianyu, Y.; Wang, X.; Hu, D.; Zhao, Z.; Lu, N.; Xie, M.; Lei, H.; Chen, Y. *Anal. Chem.* **2018**, *90*, 4725−4732.

(13) Dong, Y.; Zheng, W.; Chen, D.; Li, X.; Wang, J.; Wang, Z.; Chen, Y. *J. Agric. Food Chem.* **2019**, *67*, 9942−9949.

(14) Xianyu, Y.; Wang, Z.; Jiang, X. *ACS Nano* **2014**, *8*, 12741−12747.

(15) Zhang, Z.; Li, T.; Sheng, Y.; Liu, L.; Wu, H. *Small* **2019**, *15*, No. 1804078.

(16) Zheng, W.; Li, H.; Chen, W.; Zhang, J.; Wang, N.; Guo, X.; Jiang, X. *Small* **2018**, *14*, No. 1703857.

(17) Mei, J.; Leung, N. L. C.; Kwok, R. T. K.; Lam, J. W. Y.; Tang, B. Z. *Chem. Rev.* **2015**, *115*, 11718−11940.

(18) Choi, J. S.; Kim, S.; Yoo, D.; Shin, T. H.; Kim, H.; Gomes, M. D.; Kim, S. H.; Pines, A.; Cheon, J. *Nat. Mater.* **2017**, *16*, 537−542.

(19) Tang, J.; Li, Y.; Song, Y.; Wu, X.; Yu, G.; Tam, K. C. *Carbohydr. Polym.* **2020**, *244*, No. 116512.

(20) He, C.; Cai, X.; Wei, S.-H.; Janotti, A.; Teplyakov, A. V. *Langmuir* **2020**, *36*, 14539−14545.

(21) Huang, Y.; Zhang, W.; Pang, S.; Chen, J.; Bhatt, P.; Mishra, S.; Chen, S. *Environ. Res.* **2021**, *194*, No. 110660.

(22) Bradley, P. M.; Journey, C. A.; Romanok, K. M.; Barber, L. B.; Buxton, H. T.; Foreman, W. T.; Furlong, E. T.; Glassmeyer, S. T.; Hladik, M. L.; Iwanowicz, L. R.; Jones, D. K.; Kolpin, D. W.; Kuivila, K. M.; Loftin, K. A.; Mills, M. A.; Meyer, M. T.; Orlando, J. L.; Reilly, T. J.; Smalling, K. L.; Villeneuve, D. L. *Environ. Sci. Technol.* **2017**, *51*, 4792−4802.

(23) Grandjean, P.; Landrigan, P. J. *Lancet Neurol.* **2014**, *13*, 330−338.

(24) Wei, J.; Chang, W.; Qileng, A.; Liu, W.; Zhang, Y.; Rong, S.; Lei, H.; Liu, Y. *Anal. Chem.* **2018**, *90*, 9606−9613.

(25) Sedgwick, A. C.; Yan, K.-C.; Mangel, D. N.; Shang, Y.; Steinbrueck, A.; Han, H.-H.; Brewster, J. T., II; Hu, X.-L.; Snelson, D. W.; Lynch, V. M.; Tian, H.; He, X.-P.; Sessler, J. L. *J. Am. Chem. Soc.* **2021**, *143*, 1278−1283.

(26) Rushing, B. R.; Selim, M. I. *Food Chem. Toxicol.* **2019**, *124*, 81−100.

(27) Caceres, I.; Al Khoury, A.; El Khoury, R.; Lorber, S.; Oswald, I.; El Khoury, A.; Atoui, A.; Puel, O.; Bailly, J. *Toxins* **2020**, *12*, 150.

(28) Marchese, S.; Polo, A.; Ariano, A.; Velotto, S.; Costantini, S.; Severino, L. *Toxins* **2018**, *10*, 214.

(29) Wu, L.; Xianyu, Y.; Wang, Z.; Dong, Y.; Hu, X.; Chen, Y. *Anal. Chem.* **2019**, *91*, 15555−15562.

(30) Xianyu, Y.; Lin, Y.; Chen, Q.; Belessiotis-Richards, A.; Stevens, M. M.; Thomas, M. R. *Angew. Chem., Int. Ed.* **2021**, *60*, 9891−9896.

(31) Sun, D.; Fan, X.; Shi, Y.; Zhang, H.; Huang, Z.; Cheng, B.; Tang, Q.; Li, W.; Zhu, Y.; Bai, J.; Liu, W.; Li, Y.; Wang, X.; Lei, X.; Chen, X. *Nat. Methods* **2021**, *18*, 107−113.